Research Article | Vol. 12, No. 5 / 1 May 2021 / Biomedical Optics Express 3037
Biomedical Optics EXPRESS

Disrupted signal variability of spontaneous neural activity in children with attention-deficit/hyperactivity disorder

ZHENYAN HU,[1,4] LU LIU,[2,3,4] MENGJING WANG,[1] GAODING JIA,[1] HAIMEI LI,[2,3] FEIFEI SI,[2,3] MIN DONG,[2,3] QIUJIN QIAN,[2,3,5] AND HAIJING NIU[1,6]

[1]*State Key Laboratory of Cognitive Neuroscience and Learning & IDG/McGovern Institute for Brain Research, Beijing Normal University, Beijing 100875, China*
[2]*Peking University Sixth Hospital/Institute of Mental Health, Beijing 100191, China*
[3]*NHC Key Laboratory of Mental Health (Peking University), National Clinical Research Center for Mental Disorders (Peking University Sixth Hospital), Beijing 100191, China*
[4]*Zhenyan Hu and Lu Liu contributed equally to this research*
[5]*qianqiujin@bjmu.edu.cn*
[6]*niuhjing@bnu.edu.cn*

Abstract: Brain signal variability (BSV) has shown to be powerful in characterizing human brain development and neuropsychiatric disorders. Multiscale entropy (MSE) is a novel method for quantifying the variability of brain signal, and helps elucidate complex dynamic pathological mechanisms in children with attention-deficit/hyperactivity disorder (ADHD). Here, multiple-channel resting-state functional near-infrared spectroscopy (fNIRS) imaging data were acquired from 42 children with ADHD and 41 healthy controls (HCs) and then BSV was calculated for each participant based on the MSE analysis. Compared with HCs, ADHD group exhibited reduced BSV in both high-order and primary brain functional networks, e.g., the default mode, frontoparietal, attention and visual networks. Intriguingly, the BSV aberrations negatively correlated with ADHD symptoms in the frontoparietal network and negatively correlated with reaction time variability in the frontoparietal, default mode, somatomotor and attention networks. This study demonstrates a wide alternation in the moment-to-moment variability of spontaneous brain signal in children with ADHD, and highlights the potential for using MSE metric as a disease biomarker.

1. Introduction

Attention-deficit/hyperactivity disorder (ADHD) is the most common neurodevelopmental disorder during childhood and adolescence, with approximately 7.2% of school-aged children meeting diagnostic criteria [1]. The children with ADHD commonly have some typical symptoms of inattention, hyperactivity and impulsivity [2], and the symptoms continue into adulthood in approximately 50% to 60% [3]. The exploration of neuropathological mechanism and development of ADHD is of significant importance.

Neuroimaging technique provides a potential tool for exploring brain function disorder in children with ADHD. Accumulating evidence has suggested dysfunction in some important brain functional connectivity and network topology in the children with ADHD. For example, Zhan et al. found the disconnection between visual and the other brain regions in children with ADHD [4]. Furthermore, it has also been found that the ADHD patients exhibited decreased global efficiency [5] and increased local efficiency [6] compared to healthy controls (HCs). These studies, from the views of large-scale network, demonstrate that brain functional organization is

#418921 https://doi.org/10.1364/BOE.418921
Journal © 2021 Received 6 Jan 2021; revised 16 Apr 2021; accepted 22 Apr 2021; published 29 Apr 2021

Biomedical Optics EXPRESS

disrupted in children with ADHD [5,7,8], which is also associated with the cognitive dysfunction of the disorder.

Recent progress in variability of moment-to-moment brain signal provided a new avenue for exploring local brain function using neuroimaging data. The approach of brain signal variability (BSV) has shown to be powerful in characterizing human brain development, neural function, cognitive performance and clinical conditions [9]. BSV depicts the magnitude of some aspects of variability from moment to moment in neuroimaging time series [9] and can be measured in forms of variance [10], standard deviation [11,12], mean square successive difference [13,14] or principle component analysis [15,16]. Another common approach to examine BSV is multiscale entropy (MSE, [17,18]) that quantifies signal complexity or temporal predictability in a time series [15,16]. The benefit of MSE measure is that it provides a profile of entropy across multiple time scales and assigns low values to both highly deterministic and completely random signals, which makes it explicit to measure signal complexity [16].

To quantify regularity and predictability of signals across multiple time scales, MSE requires a relatively long time series that can adequately capture the scale dependency [15]. As a novel imaging tool, functional near-infrared spectroscopy (fNIRS) is suitable for MSE analysis due to its relatively long temporal information and high sampling rate ($\geq$ 10Hz) [19,20]. Furthermore, fNIRS is an ideal brain imaging tool for children with ADHD because of its natural imaging environment, portability, and tolerance for subtle head motion [19–21]. Notably, fNIRS has been previously used in exploring the neural basis underlying different cognitive demands in ADHD, such as inhibition [22], working memory [23], cognitive flexibility [24], attention [25], and emotion regulation [26]. However, since most fNIRS studies focused on the task-associated brain activation of ADHD, the investigations of intrinsic brain activity in ADHD are relatively few. Further, how the variability of brain signals was associated with the symptoms of children with ADHD remains unexplored. Recently, resting state, as an important experimental paradigm, has been introduced to fNIRS studies. The resting state is a natural imaging condition in which there is neither overt perceptual input nor behavioral output. Compared to traditional task-associated brain activation, the resting-state fNIRS (rs-fNIRS), which measures spontaneous or intrinsic neural activity in brain, can generate comparable results across different studies. Meantime, the operating procedure is relatively easy for both researchers and participants. With the resting-state fNIRS imaging, one of our previous studies has revealed that the elderly patients exhibited decreased MSE compared to HCs [27], which demonstrated the potential of fNIRS imaging technique and this MSE analysis in children with ADHD.

ADHD has been classified as a neurodevelopmental disorder in the Diagnostic and Statistical Manual of Mental Disorders fifth edition (DSM-5) [2]; what's more, both imaging and neuropsychological studies have indicated delayed maturation in ADHD [28,29]. Meanwhile, brain signal variability is widely accepted that it increases with typical development [30]. Based on the theories mentioned above, we aimed to apply MSE analyses of fNIRS data to investigate the BSV in children with ADHD. We hypothesized that children with ADHD would show decreased BSV compared with age-matched healthy children, and that such variability could be associated with ADHD symptoms and cognitive dysfunction.

2. Materials and methods

2.1. Participants

Forty-two boys with ADHD (aged 8 to 12 years old, Mean $\pm$ SD = 9.4 $\pm$ 1.1) were recruited from the clinics of Peking University Sixth Hospital/Institute of Mental Health. The diagnosis of ADHD was determined by an experienced psychiatrist using the Clinical Diagnostic Interview Scale (CDIS) [31,32] in a semi-structured interview according to the criteria of the Diagnostic and Statistical Manual of Mental Disorders, Fourth Edition. The inclusion criteria were as follows: 1) right-handedness; 2) full scale estimated IQ using the Chinese Wechsler Intelligence

Biomedical Optics EXPRESS

Scale for Children [33] ≥ 80; 3) medication-naïve (stimulant and non- stimulant medications) and free of other medical interventions. Patients with a diagnosis of schizophrenia, pervasive developmental disorders, bipolar disorder, epilepsy, mental retardation, or other brain disorders were excluded. It should be noted that this study only focused on boys with ADHD considering that ADHD is more frequently prominent in males with a male-to-female ratio of 4:1 in clinical samples [34].

Forty-one age-matched healthy control boys (aged 8 to 11 years old, Mean ± SD = 9.5 ± 0.8) were enrolled from a primary school in the local community. Individuals with ADHD, mania, bipolar disorder, other major psychiatric disorders, family history of psychosis, and severe physical diseases were excluded.

This study was approved by the Medical Research Ethics Committee of Peking University Sixth Hospital. Written informed consent was obtained from the parents of all participants (and participants themselves if they were at least 10 years old) before the experiment.

2.2. Diagnoses and assessment

In addition to the clarification of an ADHD diagnosis, the CDIS was also used to assess ADHD subtypes and evaluate comorbidities. Among the recruited boys with ADHD, 22 (52.4%) met the criteria for the predominantly inattentive subtype (ADHD-I), and 20 (47.6%) met the criteria for the combined subtype (ADHD-C) (Table 1). Regarding comorbidities, 8 (19.0%) had disruptive behavior disorder (DBD), including 7 (16.7%) with oppositional defiant disorder (ODD) and 1 (2.4%) with DBD-not otherwise specified (DBD-NOS); 1 (2.4%) had social phobia, 1 (2.4%) had major depression disorder, 8 (19.0%) had a tic disorder, and 19 (45.2%) had a learning disorder.

Table 1. Demographic and clinical characteristics of ADHD and HCs

Characteristics	ADHD (n=42)	HCs (n=41)	*T* value	*P* value
Age in years (Mean ± SD)	9.4 ± 1.1	9.5 ± 0.8	-0.23	0.819 [a]
IQ (Mean ± SD)	110.3 ± 13.5	115.3 ± 11.6	-1.80	0.076 [a]
ADHD subtype (n, %)				
ADHD-I	22 (52.4)	—	—	—
ADHD-C	20 (47.6)	—	—	—
ADHD symptoms (Mean ± SD)				
Inattentive	17.8 ± 3.2	8.8 ± 4.7	10.32	<0.001 [a]
Hyperactive/Impulsive	12.7 ± 6.0	7.3 ± 4.5	4.66	<0.001 [a]
Total	30.6 ± 7.8	16.1 ± 8.5	8.09	<0.001 [a]

Abbreviations: ADHD, attention-deficit/hyperactivity disorder; HCs, healthy controls; SD, standard deviation; IQ, intelligence quotient; ADHD-I, ADHD inattentive subtype; ADHD-C, ADHD combined subtype.
[a]The *P* value was obtained using two-sample t-test.

The cognitive function was assessed using the reaction time variability (RTV) index adopted from a Stop Signal Task in the Cambridge Neuropsychological Test Automated Battery (CANTAB). Each participant was asked to complete a 20-min task, in which the participant must respond to an arrow stimulus by selecting one of two options, depending on the direction at which the arrow points. The RTV was calculated as the ratio of standard deviation to mean value of the reaction time for correct responses for analyses [35]. The RTV data were only available for 39 ADHD patients (21 ADHD-I and 18 ADHD-C) and 24 HCs.

2.3. Data acquisition

A multichannel near-infrared optical imaging system (Hui Chuang, China) with continuous waves and a 17 Hz sampling rate was used to collect rs-fNIRS data. Similar to our previous study

Biomedical Optics EXPRESS

[5], twenty-four light sources (each with two wavelengths: 670 and 830 nm) and twenty-eight detectors were arranged on the participant's head, with adjacent source and detector pairs being 3 cm apart and composed of 80 different measurement channels (Fig. 1(A)). Using the external auditory canals and vertex of the participants as landmarks, the position of these probes was established according to the international 10-20 system. Specifically, measurement channels 35 and 36 were placed around T3 and T4, and the midpoint of the two channels was localized in Cz (Fig. 1(B)). Considering changes of the averaged head circumference from 51.5 cm in 8-years-old children to 53.2 cm in 12-years-old children [36], we estimated the measurement inconsistency across participants was in the range of 0.09 cm (i.e., [(53.2-51.5)/53.2] × 3 cm; 3cm is the S-D separation). The positions of the measurement channels were validated by the spatial coordinates, which were acquired from the structural MRI image of an arbitrary participant with a Siemens 3.0 Tesla scanner. The channels were labeled with vitamin E capsules during structural MRI scanning and were projected on the network templates from Yeo et al. [37] in further analyses. According to the templates, six functional networks, i.e., default mode (DMN), frontoparietal (FPN), ventral attention (VAN), somatomotor (SMN), dorsal attention (DAN) and visual (VN) networks, were involved and displayed with different colors in our study (Fig. 1(C)).

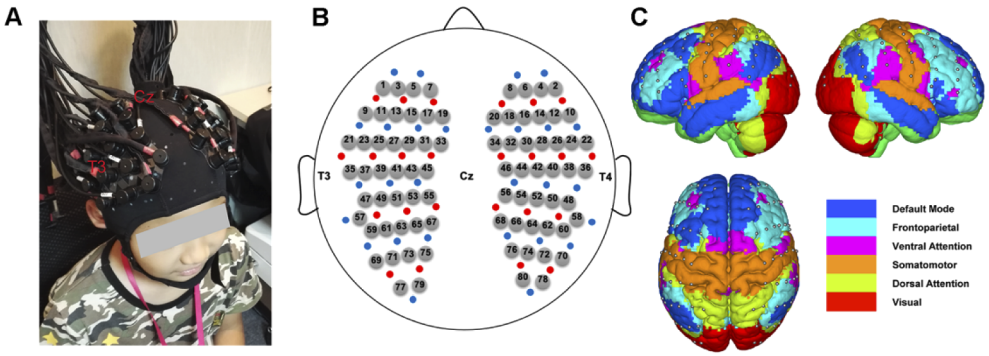

Fig. 1. Schematic illustration of experimental data collection. (A) Photograph of fNIRS data collection from a participant. (B-C) The arrangement of the whole-head 80 measurement channels on a structural brain template, the red and blue dots represent the sources and detectors, respectively. (B) and a functional network template (C) [37].

2.4. Data preprocessing

The in-house FC-NIRS package (http://www.nitrc.org/projects/fcnirs [19]) was used to preprocess the current resting-state fNIRS data in this study. First, motion artifacts were examined and removed from the optical signals using a spline interpolation method [38]. This method detected the motion-induced artifacts by calculating moving standard deviation (MSD) within sliding time windows in a window length of 2 seconds. The MSD values larger than a predefined threshold (e.g., 5 MSD [19]) were regarded as artifacts. The time series that represented the motion artifacts was further modeled via a cubic spline interpolation, which was then subtracted from the original signal of the time series. The resulting signal was considered to be free of motion artifacts. Next, the signals were bandpass filtered with a frequency of 0.01 Hz-0.1 Hz [39] to diminish the interference of low-frequency drift and high-frequency neurophysiological noise [40]. Subsequently, they were transformed into the concentrations of oxyhemoglobin (HbO) and deoxyhemoglobin (HbR) using the modified Beer-Lambert law [41] with a differential path-length factor of 6 for two wavelengths [41–45]. Finally, an eight-minute stable hemoglobin time series was extracted from each participant. Note that the HbO data were used for subsequent analysis considering its better signal-to-noise ratio [46].

Biomedical Optics EXPRESS

2.5. Multiscale entropy and brain signal variability

The multiscale entropy (MSE) algorithm, which has been widely used for characterizing neural signal complexity, was adopted to estimate brain signal variability (BSV) in this study. MSE was calculated according to the following steps similar to our previous research [27]. First, the HbO concentration time series $\{x_1, \ldots x_i, \ldots x_N\}$ was downsampled to obtain a coarse-grained time series for different timescales t. The coarse-grained time series $y^t$was generated by averaging the data points within nonoverlapping windows of length t. Each value of the coarse-grained time series, y_j^t, was computed using the following equation:

$$y_j^t = \frac{1}{t}\sum_{i=(j-1)t+1}^{jt} x_i,\ 1 \le j \le \frac{N}{t}\ . \tag{1}$$

x_i denotes the value of time point i in the original time series; N defines the number of time points; and j is the index of each coarse-grained time series. Second, the sample entropy of each downsampled time series, S_E, was calculated by:

$$S_E(m, r) = -\ln \frac{C_{m+1}(r)}{C_m(r)}, \tag{2}$$

where

$$C_m(r) = \frac{number\ of\ pairs(i,j)\ with\ |v_i^m - v_j^m| < r \times STD(y)}{number\ of\ all\ probable\ pairs}. \tag{3}$$

In Eqs. (2) and (3), m defines the pattern length indicating that m consecutive data points are used for pattern matching, and r specifies the similarity criterion indicating the threshold portion of the time series standard. In this study, pattern length was set to m=2 and the similarity criterion was chosen to $r = 0.2$, which were judged to be optimal and statistically valid following the method used in [27,47,48]. The data points are considered to have indistinguishable amplitude values when the absolute amplitude difference among them is lower than r. v_i^m is the vector defined as $\{v_i^m = y_i, y_{i+1}, \ldots y_{i+m-1}\}$; the definition of v_j^m is similar to that of v_i^m, and $|v_i^m - v_j^m|$ means the Chebychev distance between v_i^m and v_j^m.

MSE, the sample entropy across different temporal scales, quantifies the signal variability by estimating the predictability of amplitude patterns across a time series. While lower MSE values indicate a low complexity and a high degree of determinacy for the signal, higher MSE values reflect a high complexity and a low degree of predictability or rich information for the signal.

2.6. Statistical analysis

2.6.1. Between-group differences in brain signal variability

To evaluate group differences in BSV, the MSE values of each channel between the ADHD and HCs were compared using a multiple linear regression model, in which MSE was considered as dependent variable, group as independent variable, and age, IQ, age × group (i.e., interaction effect of age and group) and IQ × group as covariates. In the model, significant group differences were determined by P values lower than 0.05. False discovery rate (FDR) correction [49] was used to control the multiple testing error by correcting P values.

2.6.2. Correlation between brain signal variability and ADHD core symptoms/reaction time variability

Pearson correlation analyses were performed between MSE and ADHD symptom scores (inattentive, hyperactive/impulsive and total scores) as well as between MSE and RTV in the ADHD and HCs, respectively. Before the correlation analyses, the effects of age and IQ were removed by multiple linear regression. FDR correction was conducted to correct the multiple comparisons.

Biomedical Optics EXPRESS

3. Results

3.1. Demographic and core symptom

The demographic and core symptom data are presented in Table 1. There were no significant differences in age ($P = 0.819$) or IQ ($P = 0.076$) between the ADHD and HCs. The ADHD group had significantly higher inattentive scores ($P < 0.001$), hyperactive/impulsive scores ($P < 0.001$) and total scores ($P < 0.001$) than the HCs group.

3.2. Spatial distribution of brain signal variability in the ADHD and HCs

Similar to previous studies [27,47,50], the area under the curve (AUC) according to the sample entropy across different temporal scales (i.e., MSE) was adopted to evaluate brain signal variability (BSV). To obtain an intuitive visual presentation, we adopted bilinear interpolation algorithm to smooth MSE values across the whole brain. The bilinear interpolation algorithm performs interpolation calculations in both directions and can be extended from the linear interpolation between variables. Figure 2(A) shows the group-averaged MSE in ADHD and HC groups,

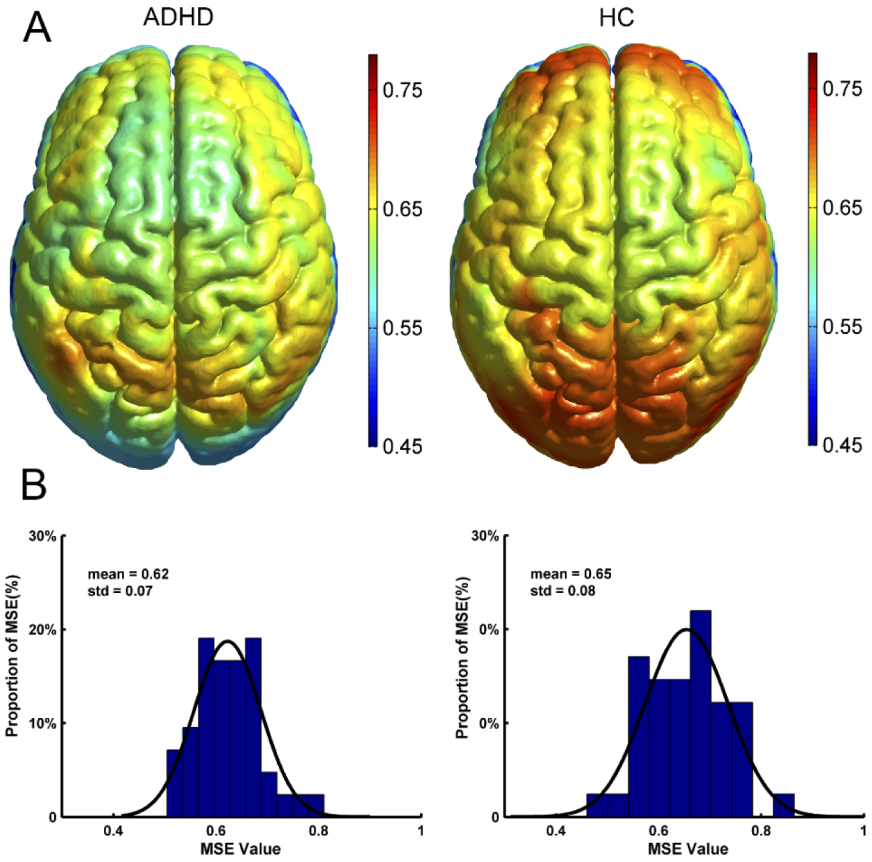

Fig. 2. MSE and its distribution. (A) The spatial maps of MSE in the whole brain for the ADHD and HC groups, which were smoothed with bilinear interpolation algorithm and implemented in MATLAB. The red color indicating higher MSE values and the blue color indicating lower MSE values. (B) Histogram distribution of MSE values among participants. The MSE distributions of both the ADHD and HC groups display approximately normal configurations.

Biomedical Optics EXPRESS

respectively. We found that the ADHD and HC groups showed similar spatial distributions in MSE, with large values located in regions of frontal, parietal and occipital cortices (Fig. 2(A)). However, quantitatively, the MSE values in ADHD were much smaller than those in HCs. The mean MSE values were 0.62 ± 0.07 (mean and standard deviation) for ADHD patients and 0.65 ± 0.08 for HCs (Fig. 2(B)).

3.3. Statistical difference in brain signal variability between ADHD and HCs

Group statistical differences in MSE between ADHD and HC were shown in Fig. 3. Specifically, MSE values on 23 measurement channels, mostly involving the default mode (DMN), frontopatietal (FPN), visual (VN), ventral (VAN) and dorsal (DAN) networks, were significantly reduced in the ADHD group (Fig. 3(A)), while two channels in default mode-network still showed significantly increased MSE values in ADHD patients (P values < 0.05, FDR correction) (Fig. 3(B)). Significant MSE differences in measurement channels between ADHD and HCs were included in Table S1 in the supplementary material.

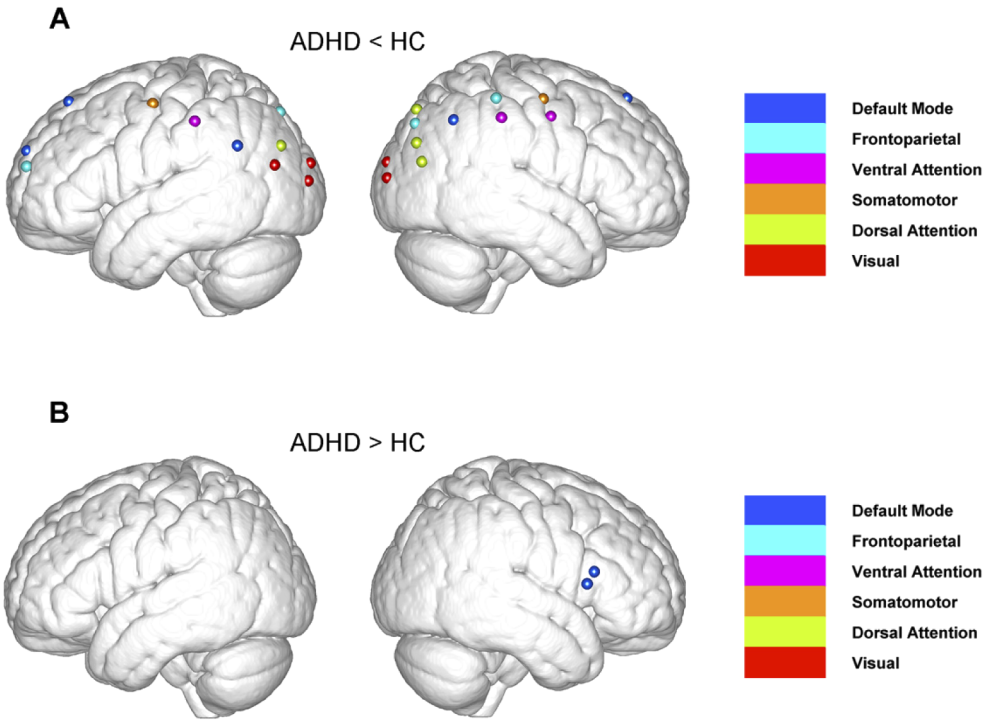

Fig. 3. Group difference analysis of MSE in different channels. (A) The measurement channels with significantly decreased MSE for ADHD participants compared to HCs ($P < 0.05$, FDR correction). (B) The measurement channels with significantly increased MSE for ADHD participants compared to HCs ($P < 0.05$, FDR correction).

3.4. Correlation between brain signal variability and ADHD core symptoms/reaction time variability

Figure 4(A) shows the Pearson correlation between MSE values and core symptoms in the ADHD group, in which the effects of age and IQ were regressed. A significantly negative correlation with hyperactive/impulsive scores ($r = -0.41$; $P = 0.007$; $P = 0.044$, FDR correction) and a marginally negative correlation with total scores ($r = -0.37$; $P = 0.017$; $P = 0.102$, FDR

Biomedical Optics EXPRESS

correction) were found in FPN, which revealed that lower brain signal variability in the FPN network was associated with more severe symptoms in the ADHD group. The above correlations were retained only in the ADHD-C subtype when the analyses were repeated in the two subtypes separately (r = -0.54; P = 0.014; P = 0.085, FDR correction for hyperactive/impulsive scores; r = -0.47; P = 0.038; P = 0.230, FDR correction for total scores, respectively).

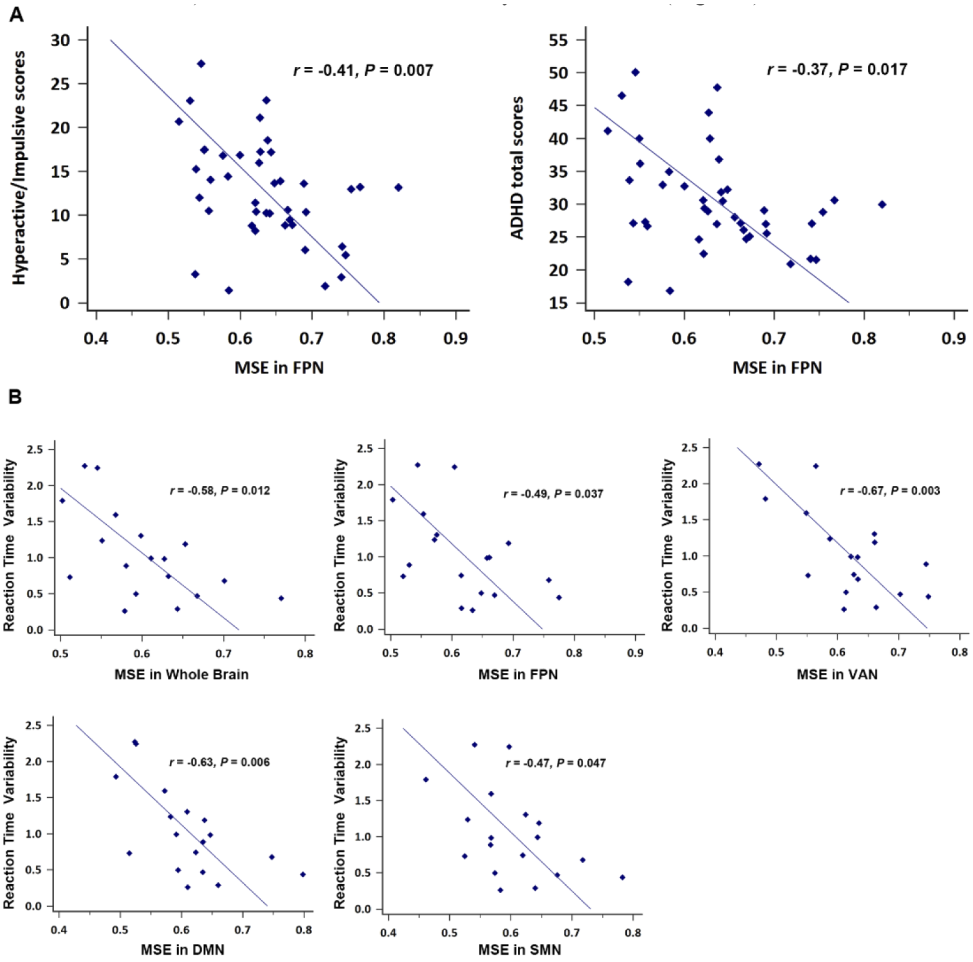

Fig. 4. Correlation of brain signal variability with core symptoms and reaction time variability. (A) Pearson correlation between brain signal variability and core symptoms after regressing age and IQ**.** (B) Pearson correlation between brain signal variability and reaction time variability after regressing age and IQ in the ADHD-C group

Increased reaction time variability (RTV) was found in ADHD patients compared to that in HCs [(0.92 ± 0.67) versus (0.39 ± 0.15), t = 3.98, P = 1.9E-04]. The above difference was also found in both ADHD-I [(0.83 ± 0.66) versus (0.39 ± 0.15), t = 3.21, P = 0.003) and ADHD-C participants [(1.03 ± 0.68) versus (0.39 ± 0.15), t = 5.01, P = 1.1E-05]. For the correlation between RTV and MSE values, no significant association was found in the whole ADHD group or in HCs. When analyzing ADHD subtypes, a negative correlation was found between MSE in the whole brain (r = -0.58, P = 0.012), VAN (r = -0.67; P = 0.003; P = 0.015, FDR correction), DMN (r = -0.63; P = 0.006; P = 0.017, FDR correction), FPN (r = -0.49; P = 0.037; P = 0.074,

Biomedical Optics EXPRESS

FDR correction), somatomotor (SMN) (r = -0.47; P = 0.047; P = 0.070, FDR correction) and reaction time variability in ADHD-C (Fig. 4(B)).

4. Discussion

In our present study, we used multiscale entropy (MSE) analysis to evaluate fNIRS signal variability in children with ADHD and typically developed controls. As we expected, categorical analyses indicated decreased brain signal variability (BSV) measured by MSE in boys with ADHD compared with age-matched healthy controls. Further quantitative analyses showed a negative association between altered MSE values and ADHD core symptoms, indicating lower BSV in the frontoparietal (FPN) network associated with more severe hyperactive/impulsive symptoms. Another important and interesting finding was that decreased BSV was negatively associated with increased reaction time variability (RTV) in children with ADHD.

Despite conflicts, strong evidence from recent studies has indicated that signal variability might increase with maturation. In the study by [16], the authors used two measures to evaluate BSV: principal component analysis (PCA) and MSE; both indicated increased brain variability with maturation from childhood (8-9 years old) to young adulthood (20-33 years old). When extending the analysis to include healthy aging, the authors found an inverted U-shaped curve with the development of BSV from childhood to old age [51]. For our present study, we focused on children with ADHD and healthy controls aged 8-12 years old. As supported by a previous study [16,52], BSV should increase with maturation. ADHD has been considered a neurodevelopmental disorder with delayed maturation in brain development. Briefly, a marked delay of approximately 3 years of cortical maturation was found in ADHD, with the most prominent delay in the prefrontal regions [29]. Consistent with this, Qian et al. [28] found that children with ADHD had development-related delays in inhibition and shifting functions. Considering the delayed development of ADHD and the 'increasing BSV' theory for typical developing individuals [30], our present study indicated that the MSE values in children with ADHD were indeed lower compared with HCs.

Another interesting finding is the negative correlation between decreased BSV and the increased cognitive variability (reaction time variability, RTV) in children with ADHD. The greater BSV representing well-functioning neural systems could enable the brain to respond to a task or the environment more accurately and smoothly, leading to more stable behavior or cognitive function [53]. That is, if the BSV decreases, the brain cannot process the information efficiently and quickly, leading to increased cognitive variability. This negative correlation has been confirmed in children with normal development, in which increased BSV accompanies lower behavioral variability [16]. Numerous studies have indicated increased RTV in patients with ADHD [54–56]. In fact, in a previous study, frontocentral theta-band phase variability was indicated to be closely linked with RTV in children with ADHD both phenotypically and genetically [57]. However, frontocentral theta-band phase variability does not account for the temporal disorganization of neural dynamics, while our findings indicate a correlation between moment-to-moment BSV and cognitive variability. RTV is an important index of sustained attention. Impaired sustained attention always occurred in children with ADHD [58], which was even state-independent and should be an endophenotype of ADHD [59]. Our present study provides the potential neural evidence underlying increased RTV in children with ADHD. This 'brain-behavior' relationship will also promote our understanding of the pathogenesis of ADHD. Significantly, the deficiency of sustained attention occurs not only in ADHD, but also in other psychiatric disorders, such as anxiety disorders [60] and mood disorders [61]. As such, our present finding will also provide meaningful reference for the research of other psychiatric disorders.

As for the functional brain networks, we found that the children with ADHD showed reduced BSV in both high-order (DMN, FPN, VAN and DAN) and primary brain functional networks

Biomedical Optics EXPRESS

(VN). These findings are interesting because they demonstrate a wide alternation in the moment-to-moment variability of spontaneous brain signal in children with ADHD. These results did not change when considering ADHD subtypes (Table S2). However, the quantitative analyses of ADHD symptoms only indicated the association between altered BSV in FPN and hyperactive-impulsive symptoms. The FPN has been suggested to be a flexible hub for cognitive control [62]. Dysfunction of FPN is a well-confirmed finding in the MRI study of ADHD and ADHD-related cognitive dysfunction, including impulsive symptoms [8,63] and inhibition [64]. Our current findings support the critical role of FPN in ADHD, especially the hyperactive/impulsive symptoms, on a temporal scale. The other networks revealed from the categorical analyses, including DMN, VAN, SMN, are also worthy of further exploration with respect to other behavioral domains and cognitive functions. In addition, the brain networks are not isolated but have complex and multiple connections. Therefore, the investigation of the inter-correlation of BSV among these brain networks may also be helpful to understand the neural dynamic complexity in participants with ADHD more comprehensively.

Several limitations should be considered for our current study. First, the sample size is relatively small, and we could not investigate the potentially explicit confounding effects of comorbidities on our findings. In addition, most results were marginal after corrections for multiple comparisons, which may also be due to the limited sample size. Second, we only included males for analyses, which may limit the generalization of our findings only to males. Third, we only recruited children as participants. Adults recruited in the future could enable us to better understand the age-related changes in BSV in participants with ADHD. Finally, although we adopted the spline interpolation method to remove head motion artifacts, the potential influence of head motion could still exist. Future studies are expected to combine motion-removing approaches and motion record system to eliminate the influence of head motions.

5. Conclusion

In summary, we utilized resting-state fNIRS imaging to explore the brain signal variability (BSV) in children with ADHD and estimated its association with ADHD core symptoms and cognitive function. The results revealed decreased BSV in children with ADHD compared to typically developing controls and decreased brain variability in ADHD was accompanied by increased ADHD core symptoms and disrupted cognitive function. Our results provide novel insights and potential biomarkers for the diagnosis of ADHD. Replications of these experiments in larger, independent population samples with wider age ranges are needed to confirm our preliminary findings.

Funding. National Natural Science Foundation of China (81761148026, 81873802, 81571340, 81571755); National Basic Research Program of China (2014CB846104); National Key Technology R&D Program (2015BAI13B01).

Disclosures. The authors declare no conflicts of interest.

Supplemental document. See Supplement 1 for supporting content.

References

1. R. Thomas, S. Sanders, J. Doust, E. Beller, and P. Glasziou, "Prevalence of attention-deficit/hyperactivity disorder: a systematic review and meta-analysis," Pediatrics **135**(4), e994–e1001 (2015).
2. A. P. Association, *Diagnostic and Statistical Manual of Mental Disorders (DSM-5)* (American Psychiatric Pub, 2013).
3. S. V. Faraone, J. Biederman, and E. Mick, "The age-dependent decline of attention deficit hyperactivity disorder: a meta-analysis of follow-up studies," Psychol. Med. **36**(2), 159–165 (2006).
4. C. Zhan, Y. Liu, K. Wu, Y. Gao, and X. Li, "Structural and functional abnormalities in children with attention-deficit/hyperactivity disorder: a focus on subgenual anterior cingulate cortex," Brain Connect **7**(2), 106–114 (2017).
5. M. Wang, Z. Hu, L. Liu, H. Li, Q. Qian, and H. Niu, "Disrupted functional brain connectivity networks in children with attention-deficit/hyperactivity disorder: evidence from resting-state functional near-infrared spectroscopy," Neurophotonics **7**(01), 1 (2020).

Biomedical Optics EXPRESS

6. P. Lin, J. B. Sun, G. Yu, Y. Wu, Y. Yang, M. L. Liang, and X. Liu, "Global and local brain network reorganization in attention-deficit/hyperactivity disorder," Brain Imaging and Behavior **8**(4), 558–569 (2014).
7. X. Qian, F. X. Castellanos, L. Q. Uddin, B. R. Y. Loo, S. W. Liu, H. L. Koh, X. W. W. Poh, D. Fung, C. T. Guan, T. S. Lee, C. G. Lim, and J. Zhou, "Large-scale brain functional network topology disruptions underlie symptom heterogeneity in children with attention-deficit/hyperactivity disorder," Neuroimage-Clin. **21**, 101600 (2019).
8. Y. Gao, D. Shuai, X. Bu, X. Hu, S. Tang, L. Zhang, H. Li, X. Hu, L. Lu, Q. Gong, and X. Huang, "Impairments of large-scale functional networks in attention-deficit/hyperactivity disorder: a meta-analysis of resting-state functional connectivity," Psychol. Med. **49**(15), 2475–2485 (2019).
9. D. D. Garrett, G. R. Samanez-Larkin, S. W. MacDonald, U. Lindenberger, A. R. McIntosh, and C. L. Grady, "Moment-to-moment brain signal variability: a next frontier in human brain mapping?" Neurosci. Biobehav. Rev. **37**(4), 610–624 (2013).
10. B. J. He, "Scale-free properties of the functional magnetic resonance imaging signal during rest and task," J. Neurosci. **31**(39), 13786–13795 (2011).
11. D. D. Garrett, N. Kovacevic, A. R. McIntosh, and C. L. Grady, "The importance of being variable," J. Neurosci. **31**(12), 4496–4503 (2011).
12. D. D. Garrett, N. Kovacevic, A. R. McIntosh, and C. L. Grady, "Blood oxygen level-dependent signal variability is more than just noise," J. Neurosci. **30**(14), 4914–4921 (2010).
13. A. Leo, G. Bernardi, G. Handjaras, D. Bonino, E. Ricciardi, and P. Pietrini, "Increased BOLD variability in the parietal cortex and enhanced parieto-occipital connectivity during tactile perception in congenitally blind individuals," Neural Plast. **2012**, 1–8 (2012).
14. G. R. Samanez-Larkin, C. M. Kuhnen, D. J. Yoo, and B. Knutson, "Variability in nucleus accumbens activity mediates age-related suboptimal financial risk taking," J. Neurosci. **30**(4), 1426–1434 (2010).
15. A. R. McIntosh, N. Kovacevic, S. Lippe, D. Garrett, C. Grady, and V. Jirsa, "The development of a noisy brain," Arch. Ital. Biol. **148**, 323–337 (2010).
16. A. R. McIntosh, N. Kovacevic, and R. J. Itier, "Increased brain signal variability accompanies lower behavioral variability in development," PLoS Comput. Biol. **4**(7), e1000106 (2008).
17. M. Costa, A. L. Goldberger, and C. K. Peng, "Multiscale entropy analysis of complex physiologic time series," Phys. Rev. Lett. **89**(6), 068102 (2002).
18. M. Costa, A. L. Goldberger, and C. K. Peng, "Multiscale entropy analysis of biological signals," Phys. Rev. E **71**(2), 021906 (2005).
19. J. Xu, X. Liu, J. Zhang, Z. Li, X. Wang, F. Fang, and H. Niu, "FC-NIRS: a functional connectivity analysis tool for near-infrared spectroscopy data," Biomed. Res. Int. **2015**, 1–11 (2015).
20. H. Niu, J. Wang, T. Zhao, N. Shu, and Y. He, "Revealing topological organization of human brain functional networks with resting-state functional near infrared spectroscopy," PLoS One **7**(9), e45771 (2012).
21. L. Cai, Q. Dong, and H. Niu, "The development of functional network organization in early childhood and early adolescence: A resting-state fNIRS study," Dev. Cogn. Neurosci. **30**, 223–235 (2018).
22. Y. Monden, I. Dan, M. Nagashima, H. Dan, M. Uga, T. Ikeda, D. Tsuzuki, Y. Kyutoku, Y. Gunji, D. Hirano, T. Taniguchi, H. Shimoizumi, E. Watanabe, and T. Yamagata, "Individual classification of ADHD children by right prefrontal hemodynamic responses during a go/no-go task as assessed by fNIRS," NeuroImage. Clin. **9**, 1–12 (2015).
23. A. C. Ehlis, C. G. Bahne, C. P. Jacob, M. J. Herrmann, and A. J. Fallgatter, "Reduced lateral prefrontal activation in adult patients with attention-deficit/hyperactivity disorder (ADHD) during a working memory task: a functional near-infrared spectroscopy (fNIRS) study," J. Psychiatr. Res. **42**(13), 1060–1067 (2008).
24. J. A. King, M. Colla, M. Brass, I. Heuser, and D. von Cramon, "Inefficient cognitive control in adult ADHD: evidence from trial-by-trial Stroop test and cued task switching performance," Behav. Brain Funct. **3**(1), 42 (2007).
25. P. Weber, J. Lutschg, and H. Fahnenstich, "Cerebral hemodynamic changes in response to an executive function task in children with attention-deficit hyperactivity disorder measured by near-infrared spectroscopy," J. Dev. Behav. Pediatr. **26**(2), 105–111 (2005).
26. H. Ichikawa, E. Nakato, S. Kanazawa, K. Shimamura, Y. Sakuta, R. Sakuta, M. K. Yamaguchi, and R. Kakigi, "Hemodynamic response of children with attention-deficit and hyperactive disorder (ADHD) to emotional facial expressions," Neuropsychologia **63**, 51–58 (2014).
27. X. Li, Z. Zhu, W. Zhao, Y. Sun, D. Wen, Y. Xie, X. Liu, H. Niu, and Y. Han, "Decreased resting-state brain signal complexity in patients with mild cognitive impairment and Alzheimer's disease: a multiscale entropy analysis," Biomed. Opt. Express **9**(4), 1916–1929 (2018).
28. Y. Qian, L. Shuai, R. C. Chan, Q. J. Qian, and Y. Wang, "The developmental trajectories of executive function of children and adolescents with attention deficit hyperactivity disorder," Res. Dev. Disabil. **34**(5), 1434–1445 (2013).
29. P. Shaw, K. Eckstrand, W. Sharp, J. Blumenthal, J. P. Lerch, D. Greenstein, L. Clasen, A. Evans, J. Giedd, and J. L. Rapoport, "Attention-deficit/hyperactivity disorder is characterized by a delay in cortical maturation," Proc. Natl. Acad. Sci. U. S. A. **104**(49), 19649–19654 (2007).
30. T. Takahashi, Y. Yoshimura, H. Hiraishi, C. Hasegawa, T. Munesue, H. Higashida, Y. Minabe, and M. Kikuchi, "Enhanced brain signal variability in children with autism spectrum disorder during early childhood," Hum. Brain Mapp **37**(3), 1038–1050 (2016).
31. R. A. Barkley, "Attention-deficit hyperactivity disorder," Sci. Am. **279**(3), 66–71 (1998).

Biomedical Optics EXPRESS

32. L. Yang, Y. F. Wang, Q. J. Qian, J. Biederman, and S. V. Faraone, "DSM-IV subtypes of ADHD in a Chinese outpatient sample," J. Am. Acad. Child Adolesc. Psychiatry **43**(3), 248–250 (2004).
33. Y. Gong and T. Cai, "*Chinese-Wechsler intelligence scale for children*," (Map Press Hunan, 1993).
34. S. V. Faraone, P. Asherson, T. Banaschewski, J. Biederman, and B. Franke, "Attention-deficit/hyperactivity disorder," Nat. Rev. Dis. Primers **1**(1), 15020 (2015).
35. A. Pinar, Z. Hawi, T. Cummins, B. Johnson, M. Pauper, J. Tong, J. Tiego, A. Finlay, M. Klein, B. Franke, A. Fornito, and M. A. Bellgrove, "Genome-wide association study reveals novel genetic locus associated with intra-individual variability in response time," Transl. Psychiatry **8**(1), 207 (2018).
36. A. Chirita-Emandi, G. Doros, I. J. Simina, M. Gafencu, and M. Puiu, "Head circumference references for school age children in Western Romania," Rev. Med. Chir. Soc. Med. Nat. Iasi. **119**, 1083–1091 (2015).
37. B. T. Yeo, F. M. Krienen, J. Sepulcre, M. R. Sabuncu, D. Lashkari, M. Hollinshead, J. L. Roffman, J. W. Smoller, L. Zollei, J. R. Polimeni, B. Fischl, H. Liu, and R. L. Buckner, "The organization of the human cerebral cortex estimated by intrinsic functional connectivity," J. Neurophysiol. **106**(3), 1125–1165 (2011).
38. F. Scholkmann, S. Spichtig, T. Muehlemann, and M. Wolf, "How to detect and reduce movement artifacts in near-infrared imaging using moving standard deviation and spline interpolation," Physiol. Meas. **31**(5), 649–662 (2010).
39. H. Niu, Z. Zhu, M. Wang, X. Li, Z. Yuan, Y. Sun, and Y. Han, "Abnormal dynamic functional connectivity and brain states in Alzheimer's diseases: functional near-infrared spectroscopy study," Neurophotonics **6**(2), 025010 (2019).
40. H. Niu, Z. Li, X. Liao, J. Wang, T. Zhao, N. Shu, X. Zhao, and Y. He, "Test-retest reliability of graph metrics in functional brain networks: a resting-state fNIRS study," PLoS One **8**(9), e72425 (2013).
41. L. Kocsis, P. Herman, and A. Eke, "The modified Beer-Lambert law revisited," Phys. Med. Biol. **51**(5), N91–N98 (2006).
42. M. Cope, D. T. Delpy, E. O. Reynolds, S. Wray, J. Wyatt, and D. Van, *Methods of Quantitating Cerebral Near Infrared Spectroscopy Data* (Oxygen Transport to Tissue X, 1988).
43. D. T. Delpy, M. Cope, P. Vanderzee, S. Arridge, S. Wray, and J. Wyatt, "Estimation of optical pathlength through tissue from direct time of flight measurement," Phys. Med. Biol. **33**(12), 1433–1442 (1988).
44. A. Sassaroli and S. Fantini, "Comment on the modified Beer-Lambert law for scattering media," Phys. Med. Biol. **49**(14), N255–N257 (2004).
45. G. Strangman, M. A. Franceschini, and D. A. Boas, "Factors affecting the accuracy of near-infrared spectroscopy concentration calculations for focal changes in oxygenation parameters," NeuroImage **18**(4), 865–879 (2003).
46. G. Strangman, J. P. Culver, J. H. Thompson, and D. A. Boas, "A quantitative comparison of simultaneous BOLD fMRI and NIRS recordings during functional brain activation," NeuroImage **17**(2), 719–731 (2002).
47. T. Takahashi, R. Y. Cho, T. Mizuno, M. Kikuchi, T. Murata, K. Takahashi, and Y. Wada, "Antipsychotics reverse abnormal EEG complexity in drug-naive schizophrenia: a multiscale entropy analysis," NeuroImage **51**(1), 173–182 (2010).
48. T. Takahashi, R. Y. Cho, T. Murata, T. Mizuno, M. Kikuchi, K. Mizukami, H. Kosaka, K. Takahashi, and Y. Wada, "Age-related variation in EEG complexity to photic stimulation: a multiscale entropy analysis," Clin. Neurophysiol. **120**(3), 476–483 (2009).
49. Y. Benjamini and Y. Hochberg, "Controlling the false discovery rate : a practical and powerful approach to multiple testing," J R Stat. Soc. B **57**, 289–300 (1995).
50. T. Mizuno, T. Takahashi, R. Y. Cho, M. Kikuchi, T. Murata, K. Takahashi, and Y. Wada, "Assessment of EEG dynamical complexity in Alzheimer's disease using multiscale entropy," Clin. Neurophysiol. **121**(9), 1438–1446 (2010).
51. A. R. McIntosh, V. Vakorin, N. Kovacevic, H. Wang, A. Diaconescu, and A. B. Protzner, "Spatiotemporal dependency of age-related changes in brain signal variability," Cereb Cortex **24**(7), 1806–1817 (2014).
52. B. Misic, T. Mills, M. J. Taylor, and A. R. Mcintosh, "Brain noise is task dependent and region specific," J. Neurosci. **104**(5), 2667–2676 (2010).
53. D. D. Garrett, A. R. McIntosh, and C. L. Grady, "Brain signal variability is parametrically modifiable," Cereb Cortex **24**(11), 2931–2940 (2014).
54. S. L. Karalunas, C. L. Huang-Pollock, and J. T. Nigg, "Is reaction time variability in ADHD mainly at low frequencies?" J. Child Psychol. Psychiatry **54**(5), 536–544 (2013).
55. M. J. Kofler, M. D. Rapport, D. E. Sarver, J. S. Raiker, S. A. Orban, L. M. Friedman, and E. G. Kolomeyer, "Reaction time variability in ADHD: a meta-analytic review of 319 studies," Clin. Psychol. Rev. **33**(6), 795–811 (2013).
56. L. Tamm, M. E. Narad, T. N. Antonini, K. M. O'Brien, L. W. Hawk Jr., and J. N. Epstein, "Reaction time variability in ADHD: a review," Neurotherapeutics **9**(3), 500–508 (2012).
57. G. McLoughlin, J. A. Palmer, F. Rijsdijk, and S. Makeig, "Genetic overlap between evoked frontocentral theta-band phase variability, reaction time variability, and attention-deficit/hyperactivity disorder symptoms in a twin study," Biol. Psychiatry **75**(3), 238–247 (2014).
58. W. Cai, S. L. Warren, K. Duberg, B. Pennington, S. P. Hinshaw, and V. Menon, "Latent brain state dynamics distinguish behavioral variability, impaired decision-making, and inattention," Mol Psychiatry (2021).
59. P. Thomson, N. Vijayakumar, K. A. Johnson, C. B. Malpas, E. Sciberras, D. Efron, P. Hazell, and T. J. Silk, "Longitudinal trajectories of sustained attention development in children and adolescents with ADHD," J. Abnorm. Child Psych. **48**(12), 1529–1542 (2020).

Biomedical Optics EXPRESS

60. T. N. Day, L. J. Chong, and A. Meyer, "Parental presence impacts a neural correlate of anxiety (the late positive potential) in 5-7 year old children: interactions with parental sensitivity to child anxiety," J. Abnorm Child Psychol. **48**(7), 951–963 (2020).
61. H. Yu, M. L. Li, Y. Meng, X. J. Li, W. Wei, Y. F. Li, L. Li, W. Guo, Q. Wang, W. Deng, X. Ma, J. Coid, and T. Li, "Inferior frontal gyrus seed-based resting-state functional connectivity and sustained attention across manic/hypomanic, euthymic and depressive phases of bipolar disorder," J. Affect Disord. **282**, 930–938 (2021).
62. S. Marek and N. U. F. Dosenbach, "The frontoparietal network: function, electrophysiology, and importance of individual precision mapping," Dialogues Clin. Neurosci. **20**(2), 133–140 (2018).
63. H. Y. Lin, W. Y. I. Tseng, M. C. Lai, K. Matsuo, and S. S. F. Gau, "Altered resting-state frontoparietal control network in children with attention-deficit/hyperactivity disorder," J. Int. Neuropsych. Soc. **21**(4), 271–284 (2015).
64. W. Cai, K. Griffiths, M. S. Korgaonkar, L. M. Williams, and V. Menon, "Inhibition-related modulation of salience and frontoparietal networks predicts cognitive control ability and inattention symptoms in children with ADHD," Mol Psychiatry (2019).